PaSTS
An Operational Dataset for Domestic Solar Thermal Systems

Florian Ebmeier
University of Tübingen
Tübingen, Germany
florian.ebmeier@uni-tuebingen.de

Nicole Ludwig
University of Tübingen
Tübingen, Germany
nicole.ludwig@uni-tuebingen.de

Georg Martius
University of Tübingen
Tübingen, Germany
Max Planck Institute for Intelligent Systems
Tübingen, Germany
georg.martius@uni-tuebingen.de

Volker H. Franz
University of Tübingen
Tübingen, Germany
volker.franz@uni-tuebingen.de

ABSTRACT
Solar thermal systems play an important role in the decarbonization of the domestic heating sector, yet there exist no publicly available datasets of such systems. Therefore, this paper presents the PaSTS dataset, a unique collection of operational data from domestic Solar Thermal Systems (STS) manufactured by Ritter Energie and marketed under the Paradigma brand. Unlike previous research that primarily relied on simulated or unpublished experimental data, this dataset is derived from the service team at Ritter Energie, offering a realistic reflection of the challenges commonly faced in the field. This paper provides a comprehensive dataset overview, emphasizing its application in anomaly and fault detection tasks within STS and establishes the dataset as the first of its kind.

Given the inherent complexities of fault detection in STS, we elaborate on the expert system-based fault detection mechanism currently in use and advocate for applying semi-supervised or unsupervised anomaly detection techniques tailored to the dataset's characteristics.

CCS CONCEPTS
• **Computing methodologies** → **Anomaly detection**; • **Hardware** → **Renewable energy**.

KEYWORDS
solar thermal systems, dataset, anomaly detection, fault detection

ACM Reference Format:
Florian Ebmeier, Nicole Ludwig, Georg Martius, and Volker H. Franz. 2024. PaSTS An Operational Dataset for Domestic Solar Thermal Systems. In *The 15th ACM International Conference on Future and Sustainable Energy Systems (E-Energy '24), June 04–07, 2024, Singapore, Singapore*. ACM, New York, NY, USA, 6 pages. https://doi.org/10.1145/3632775.3662159

E-Energy '24, June 04–07, 2024, Singapore, Singapore

ACM ISBN 979-8-4007-0480-2/24/06
https://doi.org/10.1145/3632775.3662159

1 MOTIVATION
In the realm of renewable energy, it is imperative to diversify approaches to reduce the carbon footprint of our energy sector. Notably, the heating sector – a critical component often overlooked in discussions about energy consumption – demands attention. Specifically, space and water heating represent a significant portion of energy usage, accounting for 78.9% of European households' final energy consumption [5]. Solar Thermal Systems (STS) are a promising technology to reduce the carbon footprint of the heating sector, offering a means to generate heat with minimal emissions.

However, optimizing the performance of STS presents a challenging problem. This is particularly true for domestic systems, which are prone to issues stemming from improper installation, operational faults, and general optimization challenges due to system design. These problems are documented in various studies, highlighting the need for effective solutions to enhance system reliability and efficiency [2, 6, 10, 11, 13, 14]. In response to these challenges, two primary strategies have been identified. Either simulate data using simulation programs such as TRNSYS 18 [8] or use operational data from existing systems. Specifically, in the case of operational data from existing systems, we observe a gap in the availability of public operational datasets for domestic STS, limiting research efforts in this field, with only a single year of operational data from a large-scale system currently available [16].

To bridge this gap, we introduce the Paradigma Solar Thermal Systems (PaSTS) dataset. A time series dataset encompassing data from various domestic systems managed by Ritter Energie- und Umwelttechnik GmbH & Co. KG, 72135 Dettenhausen, Germany, operating under the Paradigma brand name. By making this dataset available, we aim to facilitate data-driven approaches in the optimization and fault detection of STS, contributing to the broader goal of enhancing the sustainability of the heating sector.

2 SOLAR THERMAL SYSTEMS
Solar thermal systems are recognized as a renewable source of heat energy, particularly effective for domestic heating purposes. This section explores the operation of domestic solar thermal systems,

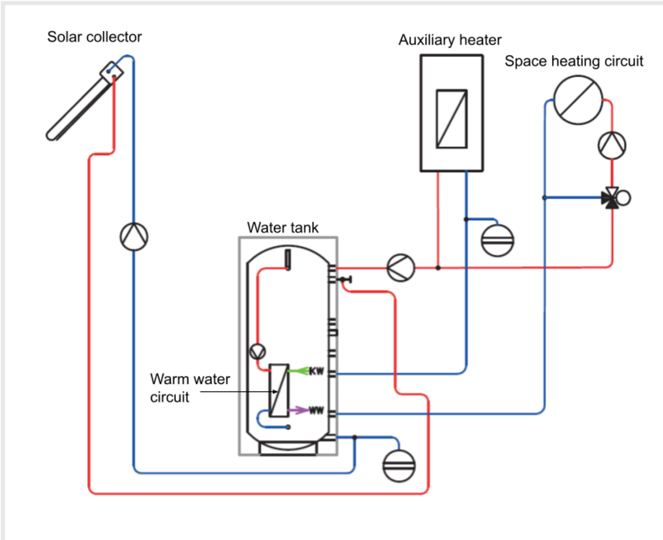

Figure 1: Example Blueprint of a Solar Thermal System. Warm water runs through red, and cold water through blue lines. The system includes a collector, a water tank, an auxiliary heater, a warm water circuit (shown inside the tank), and a space heating circuit.

which consist fundamentally of three primary components: the tank, the collector, and the control system.

(1) **The Collector**: Essential for the absorption of solar radiation, it contains a fluid that captures solar energy and converts it into heat. Usually, this liquid is some form of freeze-resistant solution. However, as Ritter Energie uses a specialized frost protection mechanism, they can use regular water, improving efficiency and reducing the need for maintenance.
(2) **The Tank**: Acts as the reservoir for the heated water, which is then utilized for domestic applications such as warm water and space heating. One important aspect of the tank is that its water must be stratified for optimal efficiency, i.e. there should not be any circulation within the tank. This is a major factor in the efficiency of the system and a large topic of research in the field [7].
(3) **The Control System**: A system consisting of various valves, a pump and a digital controller that manages the flow of the heat transfer fluid and the operation of the pump to maximize the system's efficiency. It controls all automatic valves and may be integrated with other heating or house infrastructure parts, such as auxiliary heating and freshwater mixing.

An example diagram for a system designed by Paradigma can be seen in Figure 1.

The operational principle is both simple and efficient. Upon the fluid in the collector reaching a temperature higher than that of the water in the tank, a pump is activated. This pump circulates the water through the tank, transferring heat from the collector into the tank. Possible faults in installation and design are often attributed to oversights due to overly complicated systems, see e.g. [10].

To ensure optimal functionality, the controller relies on accurate measurements of the collector temperature, ambient temperature, water tank temperature, and temperatures at all inlets and outlets. In contrast to most existing systems, the Paradigma systems also measure the volumetric flow rate of the heat transfer fluid. This data is pivotal in determining the system's energy yield and offers a detailed perspective on its efficiency and performance.

3 DATASET DESCRIPTION

The dataset comprises time series data from various domestic Solar Thermal Systems. It encompasses data from 83 systems, with operational durations ranging from 1 to 3329 days. In total, there are 39, 878 days, of which 7, 987 days have an anomaly indication and 2, 123 days have a fault indication. Anomaly and fault indications are given by the controller, where an anomaly indication marks unusual behavior potentially leading to a fault and fault indications mark faults requiring intervention. The full dataset is available under https://zenodo.org/records/11093493.

These systems exhibit diverse configurations, including variations in collector area, storage volume of the water tank, living space square meters, and the number of residents, leading to substantially different load profiles. However, most of these parameters are not included in the dataset, making them unknown to the user. For newer systems, an automatic test approximates the solar collector area, which we report in Table A1 along with more information on each system.

This scenario mirrors the reality of many existing systems, where detailed configurations are often incomplete or unknown when monitoring a system. The dataset originates from Ritter Energie's service team, capturing instances of systems affected by improper installation, suboptimal design choices, and other issues. The dataset consists of systems that are running operationally in domestic settings, often for many years. It includes "run to failure" scenarios, where systems operated effectively for an extended period before failing due to maintenance neglect, chance, or other reasons. The dataset also contains faultless systems within normal operational parameters.

It is important to note that the dataset does not represent a comprehensive sample of Ritter Energie's products but rather a collection emphasizing systems with operational issues alongside some nominal systems. This selection criterion naturally elevates the fault/anomaly rate in the dataset compared to the general population of installations.

Additionally, the systems from Ritter Energie can measure the volumetric flow, enabling the system's energy yield calculation. This feature allows for the training of machine learning models [3, 4] to estimate a system's energy yield and load profile. Many older systems and systems by other manufacturers, which do not measure these values directly, rely on approximations based on temperature differentials and control signals. Assuming nominal pump flow rates, such approximations are particularly error-prone when system faults occur. A pump's gradual degradation or complete failure could lead to misleadingly high-performance approximations, falsely identifying a failing system as highly efficient.

In addition to the anomaly detection focus, this dataset is a foundational resource for developing data-driven models to estimate energy yield, a critical metric for assessing system health, maintenance needs, and the presence of faults. Therefore, establishing a reliable estimation method for systems without specific sensors is of great value.

3.1 Data

The data is provided with full days of data, capturing a data point for every minute of the day. Given that the smallest continuous time series in the dataset constitutes a day, consisting of 1440 minutes, it is recommended to analyze full days of data at a time. All systems are located in the south of Germany across various unspecified locations. Notably, the dataset does not incorporate weather-related data beyond the ambient temperature.

The dataset encompasses four distinct types of data:

- **Index:** This category encompasses the date and time of each data point along with the system identifier.
- **Sensor:** This includes all directly measured data, predominantly temperature readings, the volumetric flow rate and the system's energy yield.
- **Control signals:** These signals represent the control inputs directed towards various system components, such as the pump's control signal.
- **Status:** The dataset contains various status signals, some of which may signify the presence of a fault or other conditions derived from measurements. Additional status signals indicate the current operational mode of the system.

A comprehensive listing of all available data columns is provided in Table 1.

3.2 Data Preprocessing

Data measurements are susceptible to various disturbances, such as noise, minor anomalies, or power outages, leading to occasional gaps in the data. Furthermore, discrepancies in the measurement frequency may cause slight temporal drifts. To address these issues, we resample the data to ensure uniform minute intervals throughout the day and employ front filling for all missing data points. The published dataset (https://zenodo.org/records/11093493) includes both the raw and resampled data.

An exception in this preprocessing approach is the treatment of yield data. Given that the control system of the STS maintains a consistent record of the total energy yield over its lifetime, missing data within the daily yield column is inferred from this cumulative metric. Given the typically minor extent of these gaps, interpolating between the cumulative daily yields provides a reliable approximation.

Nevertheless, any day missing more than 144 data points, equivalent to 10% of the daily data, was excluded from the dataset. This filtration criterion is based on the rationale that a day containing less than 90% of its data inherently represents an anomaly, thus rendering its identification as such relatively straightforward.

3.3 Data Distributions

An examination of the data distributions reveals that most variables in the dataset do not follow a normal distribution. As depicted in Figure 2, we analyze representative distributions from the system with the longest operational span of 3331 days. As shown in Figure 2(a), the ambient temperature approximates a normal distribution more closely than the other variables. Conversely, the collector temperature and other temperature readings, exemplified in Figure 2(b), predominantly exhibit a pronounced peak at their most frequent operational temperature, typically on the lower end of the temperature spectrum, followed by an extended tail towards higher temperatures. Notably, some systems display a minor secondary peak, mirroring the profile observed in Figure 2(b) and corresponding to stagnation, which presents no problem in these water-based STS.

Control and status variables predominantly exhibit a mode of 0, indicative of no action or default status. This trend is observable in Figures 2(c) and 2(d), with the pattern being even more pronounced across other status variables. In these cases, the predominant status typically represents a standard operation, often encoded as 0. The volumetric flow rate and pump activity also show specific ranges being significantly more common alongside less frequent outlier values. It is important to note the impact of pump and piping deterioration over time, which alters the flow rate achievable with a given control signal, resulting in shifts in the average data range for the pump's control signal values over time.

3.4 Expert System Based Fault Detection

Utilizing the dataset for anomaly detection necessitates understanding how fault indication ("sto") and anomaly indication ("Merk") indices are generated. The expert system-based fault detection in Paradigma controllers operates on a set of definitive rules. For instance, a sensor malfunction or abnormal temperature readings lead to immediate fault detection, setting the "sto" value to 1. However, many non-trivial faults do not trigger an instant fault code due to the complexity of determining an actual error.[1]

Studies highlight a significant challenge with expert systems: the propensity for false positives, where faults are detected erroneously [14]. This issue is particularly pronounced in dynamic environments, such as during the initial increase in solar radiance or amid unusual load profiles. To mitigate false positives, the expert system assigns a "Merk" value to note anomalous behavior, postponing the definitive fault classification ("sto" value set to 1) until further automatic tests have been conducted by the controller. These tests typically occur during nighttime downtimes.

Furthermore, these indications are set to 1 until the issue is fully resolved and then reset to 0. An anomaly indication ("Merk") may persist across several days without immediate anomalous behavior. This is also true for the "sto" value, which remains set until the underlying fault is rectified. Fault indications, which are often accompanied by an auditory signal, can be prematurely marked as resolved by the user, despite the fault remaining unfixed, leading to the "sto" value being erroneously reverted to 0.

4 DISCUSSION

When benchmarking an anomaly detection model on this dataset, several considerations emerge. Relying solely on the "sto" value for target indices could result in a low detection rate since this value is immediately set only in cases of clear-cut faults, such as sensor

[1] As the concrete fault detection software is not public, we cannot go into more detail here.

Table 1: Available data columns in the dataset. All data is in the system's local timezone. All systems are located in the south of Germany, at different locations.

Column	Description	Unit / Valuerange	Type
datetime	Timestamp	DD.MM.YYYY HH:MM:SS	Index
system	System Identifier	Three digit integer	Index
TSA1	Solar collector temperature	$°C$	Sensor
TSE	Collector inlet temperature	$°C$	Sensor
TW	Water tank temperature	$°C$	Sensor
TSV	Collector outlet temperature	$°C$	Sensor
TAM	Ambient Temperature	$°C$	Sensor
VF	Volumetric Flow Rate	$[l/min]$	Sensor
TE	Current day yield	[kWh]	Sensor
GE	Lifetime yield	[kWh]	Sensor
pwm	Control signal to pump	Percentage value	Control signal
ctr	Pump rate in frost protection	Percentage value	Control signal
fst	Status of frost protection	Between 0 and 4	Status
Stat	Current operation Status	Between 0 and 13	Status
diag	Status of diagnosis function	Between 0 and 15	Status
sto	Fault indication	0 or 1	Status
Merk	Anomaly indication	0 or 1	Status

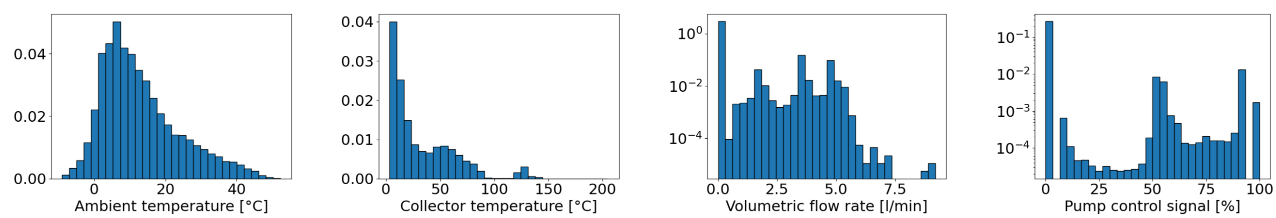

(a) (b) (c) (d)

Figure 2: Data distributions amongst different sensors are shown for the system with the longest operation time, system 902 with 3329 days. Shown are the ambient temperature (a), the collector temperature (b), the volumetric flow rate (c) and the control signal to the pump (d). Note the logarithmic scale in (c) and (d).

failures. Moreover, the anomaly indicator's nature – its persistence over time and activation during nominal but unusual system behavior – complicates its role as a reliable anomaly marker. Both indications might also persist into days without any anomalous behavior. Thus, when relying on the labels provided by the dataset, a model perfectly detecting any anomalous behavior will exhibit a large amount of false positives and false negatives. When evaluating a model on the dataset utilizing standard metrics like precision, recall, F1 score or other label-dependent metrics, exceedingly large values should warrant scrutiny to ensure no data leakage or other model issues are present. A reasonable metric consequently needs to incorporate the time-delay between the fault indication and the first occurrence of the fault, reducing false positive and false negative rates.

Anomaly detection methods can be generally separated into supervised, semi-supervised and unsupervised models [15]. Supervised models, i.e. models trained to predict the data annotation directly, require accurate targets for training. As the data annotation in this particular dataset cannot provide this, we strongly discourage the use of supervised models.

The anomaly detection challenge presented by this dataset particularly suits semi-supervised and unsupervised learning methods due to the ambiguous nature of the data annotation. While capturing a broad range of nominal behaviors, the dataset may not encompass all conceivable fault types. This uncertainty, coupled with the prohibitive costs associated with individual monitoring and explicit fault detection, underscores the potential of unsupervised anomaly detection techniques in this context, even when faced with ambiguous labels.

Semi-supervised models, such as USAD [1] or LSTM-VAE [12], are provided with training data that only contain nominal behavior and are susceptible to anomaly contamination in their training data. To adhere to the requirements of semi-supervised models, we suggest to only train them on systems with a fault rate of less than 1% and to additionally filter out any data points flagged as faults or anomalies. Unsupervised models, such as Isolation Forest [9], are independent of the data annotation and can thus accommodate anomalies within the training data.

5 CONCLUSION

PaSTS introduces a novel resource within domestic solar thermal systems to enhance the scope of anomaly detection and fault detection in this field. This dataset distinguishes itself from prior efforts by grounding its composition in operational data gathered from an extensive array of systems, offering a more authentic reflection of the data encountered in practical settings. It is thus the first dataset of operational data from domestic STS.

ACKNOWLEDGMENTS

This project was funded by the Deutsche Forschungsgemeinschaft (DFG, German Research Foundation) under Germany’s Excellence Strategy - EXC number 2064/1 - Project number 390727645. The authors thank the international Max Planck Research School for Intelligent Systems (IMPRS-IS) for supporting Florian Ebmeier. We want to thank Ritter Energie for providing us with the data on which this dataset is based.

REFERENCES

[1] Julien Audibert, Pietro Michiardi, Frédéric Guyard, Sébastien Marti, and Maria A. Zuluaga. 2020. USAD: UnSupervised Anomaly Detection on Multivariate Time Series. In *Proceedings of the 26th ACM SIGKDD International Conference on Knowledge Discovery & Data Mining (KDD ’20)*. Association for Computing Machinery, New York, NY, USA, 3395–3404. https://doi.org/10.1145/3394486.3403392

[2] A. C. de Keizer, K. Vajen, and U. Jordan. 2011. Review of long-term fault detection approaches in solar thermal systems. *Solar Energy* 85, 7 (July 2011), 1430–1439. https://doi.org/10.1016/j.solener.2011.03.025

[3] Florian Ebmeier, Nicole Ludwig, Georg Martius, and Volker H. Franz. 2022. Fault Detection in Solar Thermal Systems Using Machine Learning. (2022). Poster presented at EuroSun2022.

[4] Florian Ebmeier, Nicole Ludwig, Jannik Thuemmel, Georg Martius, and Volker H. Franz. 2024. Attention-Based Anomaly Detection in Solar Thermal Systems. (2024). Submitted to Eurosun2024.

[5] Eurostat. 2021. Disaggregated final energy consumption in households - quantities. https://ec.europa.eu/eurostat/databrowser/view/nrg_d_hhq/default/table?lang=en Accessed: 2024-03-20.

[6] Lukas Feierl, Viktor Unterberger, Claudio Rossi, Bernhard Gerardts, and Manuel Gaetani. 2023. Fault detective: Automatic fault-detection for solar thermal systems based on artificial intelligence. *Solar Energy Advances* 3, 100033 (Jan. 2023). https://doi.org/10.1016/j.seja.2023.100033

[7] YM Han, RZ Wang, and YJ Dai. 2009. Thermal stratification within the water tank. *Renewable and Sustainable Energy Reviews* 13, 5 (2009), 1014–1026.

[8] Klein, S.A. et al. 2017. *TRNSYS 18: A Transient System Simulation Program.* Solar Energy Laboratory, University of Wisconsin-Madison. http://sel.me.wisc.edu/trnsys

[9] Fei Tony Liu, Kai Ming Ting, and Zhi-Hua Zhou. 2008. Isolation forest. In *2008 eighth ieee international conference on data mining*. IEEE, 413–422.

[10] Y. Louvet, F. Pag, D. Ritter, C. Schmelzer, and K. Vajen. 2022. About common but avoidable faults during planning, installation, and operation of solar heating plants in industrial applications. *Solar Energy Advances* 2 (Jan. 2022), 100029. https://doi.org/10.1016/j.seja.2022.100029

[11] Peter Pärisch and Klaus Vanoli. 2007. Quality assurance with the ISFH-Input/Output-Procedure 6-year-experience with 14 solar thermal systems. *Proceedings of ESTEC* (2007), 315–320.

[12] Daehyung Park, Yuuna Hoshi, and Charles C Kemp. 2018. A multimodal anomaly detector for robot-assisted feeding using an lstm-based variational autoencoder. *IEEE Robotics and Automation Letters* 3, 3 (2018), 1544–1551.

[13] Christoph Schmelzer, Matthias Georgii, Janybek Orozaliev, and Klaus Vajen. 2020. Fault Detection for Solar Thermal Systems–overall system evaluation or component-oriented approach. *Proceedings of the EuroSun 2020* (2020).

[14] Christoph Schmelzer, Matthias Georgii, Christian Sauer, Janybek Orozaliev, and Klaus Vajen. 2022. Fault detection for solar thermal systems: Evaluation and improvement of existing algorithms. (2022).

[15] Sebastian Schmidl, Phillip Wenig, and Thorsten Papenbrock. 2022. Anomaly detection in time series: a comprehensive evaluation. *Proceedings of the VLDB Endowment* 15, 9 (May 2022), 1779–1797. https://doi.org/10.14778/3538598.3538602

[16] Daniel Tschopp, Philip Ohnewein, Roman Stelzer, Lukas Feierl, Marnoch Hamilton-Jones, Maria Moser, and Christian Holter. 2023. One year of high-precision operational data including measurement uncertainties from a large-scale solar thermal collector array with flat plate collectors, located in Graz, Austria. (2023). https://doi.org/10.5281/zenodo.7741084

A SYSTEM INFORMATION

Table A1 summarises the data availability, anomaly indications and faults for each solar thermal system in the dataset.

B DATA EXAMPLES

The following graphs show some examples of the temperature time series in the dataset. In Figure A1, we can see a regular spring day on 16.03.2020 for system 041. We observe the typical high frequency oscillations during the day, which is the expected behavior when exchanging hot water from the collector with cold water from the tank. The tank temperature slowly rises during the operation.

In contrast to this, we show two consecutive winter days of system 030 in Figure A2. Note the missing tank temperature sensor in this system, leading to an erroneous, constant 0 degree measurement of the tank temperature. Damage to the system led to air entering the pipes, leading to a fault in the pump and a freezing of the system on 26.02.2018. This would be considered a critical fault because a frozen system can lead to frozen pipes and water damage.

The dataset also contains further faults, like sensors jumping to implausible values or dropping to a standard value. Figure A3 shows an example of this. Here, system 049 experienced a faulty tank temperature sensor on 19.07.2019.

Table A1: Information on the individual systems with the relative fault rate calculated as the percentage of days with a fault indication over the total days.

System ID	# Days	# Anomalies	# Faults	Relative	Collector area $[m^2]$
001	397	4	2	0.5 %	
002	739	102	104	14.07 %	
003	875	80	29	3.31 %	
005	366	152	193	52.73 %	
007	516	390	47	9.11 %	
012	118	9	11	9.32 %	
013	617	3	0	0.0 %	
014	167	82	55	32.93 %	
015	805	578	74	9.19 %	
016	1	1	1	100.0 %	
023	1714	86	1	0.06 %	
025	292	28	0	0.0 %	
026	193	7	1	0.52 %	
027	270	218	14	5.19 %	
028	265	68	5	1.89 %	
029	2283	399	29	1.27 %	
030	3065	263	55	1.79 %	
031	606	187	17	2.81 %	
033	408	320	0	0.0 %	
034	2836	1689	286	10.08 %	54.0
035	216	5	0	0.0 %	
036	129	26	2	1.55 %	
037	586	586	181	30.89 %	
038	46	1	0	0.0 %	54.0
040	2513	347	43	1.71 %	
041	1974	33	2	0.1 %	
043	559	10	0	0.0 %	
044	11	8	3	27.27 %	
045	279	80	30	10.75 %	34.0
046	279	132	1	0.36 %	34.0
047	552	76	51	9.24 %	
048	310	1	5	1.61 %	
049	714	21	4	0.56 %	
050	1402	165	45	3.21 %	
051	199	5	2	1.01 %	
052	2799	65	88	3.14 %	
053	344	5	0	0.0 %	
054	405	12	75	18.52 %	
058	145	2	0	0.0 %	
059	440	258	199	45.23 %	
060	240	7	0	0.0 %	
061	115	24	7	6.09 %	
062	255	2	0	0.0 %	
063	357	35	0	0.0 %	
064	34	17	2	5.88 %	
065	405	12	75	18.52 %	
067	709	102	104	14.67 %	
068	366	152	193	52.73 %	
069	46	1	0	0.0 %	12.0
070	16	10	2	12.5 %	
072	79	6	1	1.27 %	
074	73	73	0	0.0 %	29.4
075	102	65	0	0.0 %	17.6
076	73	39	0	0.0 %	6.7
077	72	46	0	0.0 %	18.1
105	68	0	0	0.0 %	7.2
106	48	0	0	0.0 %	5.3
107	76	8	18	23.68 %	22.2
110	71	1	0	0.0 %	19.8
114	20	0	0	0.0 %	19.4
116	43	42	0	0.0 %	5.5
118	103	15	0	0.0 %	13.9
119	29	3	7	24.14 %	17.9
126	92	14	0	0.0 %	7.5
136	9	4	0	0.0 %	9.2
138	123	0	0	0.0 %	9.2
144	163	18	3	1.84 %	18.0
146	144	10	0	0.0 %	9.8
149	70	10	7	10.0 %	10.0
150	8	0	0	0.0 %	
154	65	10	1	1.54 %	
158	146	8	3	2.05 %	8.4
166	139	1	10	7.19 %	19.3
169	160	6	12	7.5 %	15.9
173	24	3	0	0.0 %	
175	157	6	0	0.0 %	8.1
179	80	0	1	1.25 %	8.9
181	145	16	3	2.07 %	17.4
193	103	27	1	0.97 %	13.4
902	3329	350	16	0.48 %	
903	162	19	2	1.23 %	
904	233	26	0	0.0 %	
905	691	295	0	0.0 %	

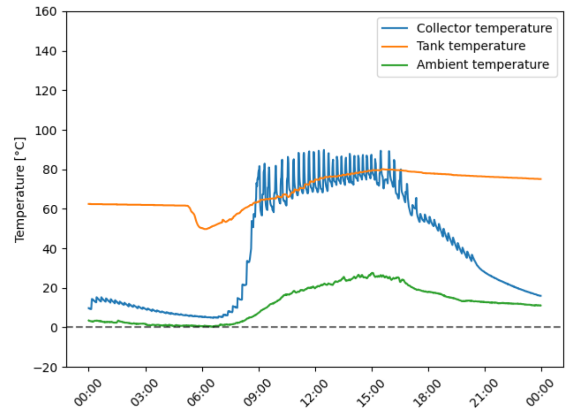

Figure A1: Example of a regular spring day in a nominal system.

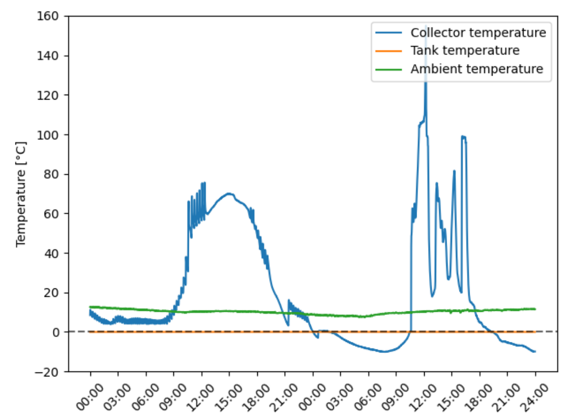

Figure A2: An unidentified incidence leading to a frozen collector would be considered a critical fault.

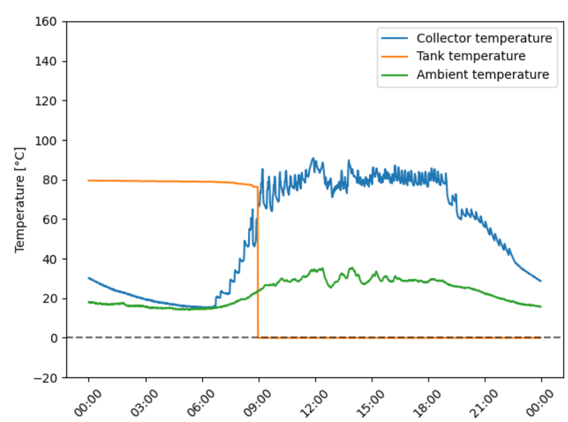

Figure A3: Tank temperature sensor suddenly drops to 0, indicating a defective sensor.